ionization potentials, electron affinities, and charge distribution, and that of Mulliken,[25] which is related to ionization potentials and electron affinities. None provides a linear free energy relationship for the reactions under discussion here. Typically, the enhancement of the rate constant caused by CH_3 substitution is underestimated compared to the predicted reduction of reactivity caused by the substitution of the electron-withdrawing halogen atoms.

The reaction transition state in the R + HI reactions, whether formed directly from the reactants or formed from a rearrangement of an R·I-H complex,[4] involves an H atom with a partial positive charge located in the region between the I atom and the methyl radical. Enhanced electron density (as provided by methyl substitution for H) at the methyl radical carbon would stabilize such a transition state and facilitate reaction, while diminished electron density (such as that caused by halogen atom substitution for H) would destabilize such a transition state. This is the behavior that is observed.

Additional studies of the kinetics of R + HI and R + HBr reactions are in progress to understand more fully the factors controlling reactivity.

Acknowledgment. We gratefully acknowledge support for this research from the National Science Foundation (Grant CHE-8996126). We thank Dr. Irene R. Slagle for her advice and assistance and Dr. Steven Stein for useful information and informative discussions. J.A.S. also thanks the Natural Science Council of the Academy of Finland and the Finnish Cultural Foundation for fellowships.

(25) Mulliken, R. S. *J. Chem. Phys.* **1934**, *2*, 782.

Ultrasonic Irradiation of *p*-Nitrophenol in Aqueous Solution

A. Kotronarou, G. Mills,† and M. R. Hoffmann*

W. M. Keck Laboratories, California Institute of Technology, Pasadena, California 91125
(Received: August 17, 1990; In Final Form: November 19, 1990)

The kinetics and mechanism of the sonochemical reactions of *p*-nitrophenol have been investigated in oxygenated aqueous solutions. In the presence of ultrasound (20 kHz, 84 W) *p*-nitrophenol was degraded primarily by denitration to yield NO_2^-, NO_3^-, benzoquinone, hydroquinone, 4-nitrocatechol, formate, and oxalate. These reaction products and the kinetic observations are consistent with a model involving high-temperature reactions of *p*-nitrophenol in the interfacial region of cavitation bubbles. The main reaction pathway appears to be carbon–nitrogen bond cleavage. Reaction with hydroxyl radical provides a secondary reaction channel. The average effective temperature of the interfacial region surrounding the cavitation bubbles was estimated to be $T \simeq 800$ K.

Introduction

The action of ultrasonic waves in liquids can induce or accelerate a wide variety of chemical reactions.[1] The chemical effects of ultrasound have been explained in terms of reactions occurring inside, at the interface, or at some distance away from cavitating gas bubbles.[1-3] In the interior of a collapsing bubble, extreme but transient conditions are known to exist. Temperatures approaching 5000 K have been determined[4] and pressures of several hundred atmospheres have been calculated.[5] Temperatures on the order of 2000 K have been determined for the interfacial region.[4] These and other important results such as the direct observation of cavitation dynamics[6] and the ESR[7] detection of H• and •OH radicals from the thermal decomposition of water have generated an increasing interest in sonochemistry. Much of the current interest in sonochemistry has arisen because of the utilization of sonolysis in catalysis[1] and synthesis.[8]

Sonochemical reactions are characterized by the simultaneous occurrence of pyrolysis and radical reactions especially at high solute concentrations.[9] Any volatile solute will participate in the former reactions because of its presence inside the bubbles during the oscillations or collapse of the cavities.[9-11] In the solvent layer surrounding the hot bubble, both combustion and free-radical reactions (e.g., involving •OH derived from the decomposition of H_2O) are possible. Pyrolysis (i.e., combustion) in the interfacial region is predominant at high solute concentrations,[11a,12] while at low solute concentrations free-radical reactions are likely to predominate.[12] In the bulk solution phase the reaction pathways are similar to those observed in aqueous radiation chemistry.[11a-13] However, evidence for combustion reactions at low solute concentrations with nonvolatile surfactants and polymers has been presented.[14]

In this paper we present kinetic data and selected mechanistic observations for the sonochemical degradation of *p*-nitrophenol (PNP) in water. We were motivated in part by the potential application of sonolysis for the elimination of chemical contam-

* To whom correspondence should be addressed.
† Present address: Department of Chemistry, Auburn University, Auburn, AL 36849.

(1) Suslick, K. S. In *Ultrasound: Its Chemical, Physical and Biological Effects*; Suslick, K. S., Ed.; VCH: New York, 1988; pp 126-163.
(2) Sehgal, C. M.; Wang, S. Y. *J. Am. Chem. Soc.* **1981**, *103*, 6606.
(3) Henglein, A. *Ultrasonics* **1987**, *25*, 6.
(4) Suslick, K. S.; Hammerton, D. A.; Cline, D. E., Jr. *J. Am. Chem. Soc.* **1986**, *108*, 5641.
(5) Shutilov, V. A. *Fundamental Physics of Ultrasound*; Gordon & Breach Science Publishers: New York, 1988.
(6) Lauterborn, W. *Acustica* **1974**, *31*, 51.
(7) (a) Makino, K.; Massoba, M. M.; Riesz, P. *J. Phys. Chem.* **1983**, *87*, 1369. (b) Makino, K.; Massoba, M. M.; Riesz, P. *J. Am. Chem. Soc.* **1982**, *104*, 3537.
(8) Suslick, K. S. In *Modern Synthetic Methods*; Sheffold, R., Ed.; Springer-Verlag: New York, 1986; Vol. 4.
(9) Henglein, A.; Kormann, C. *Int. J. Radiat. Biol.* **1985**, *48*, 251.
(10) (a) Murali Krishna, C.; Kondo, T.; Riesz, P. *J. Phys. Chem.* **1989**, *93*, 5166. (b) Murali Krishna, C.; Lion, Y.; Kondo, T.; Riesz, P. *J. Phys. Chem.* **1987**, *91*, 5847.
(11) (a) Hart, E. J.; Fischer, Ch.-H.; Henglein, A. *J. Phys. Chem.* **1986**, *90*, 5989. (b) Fischer, Ch.-H.; Hart, E. J.; Henglein, A. *J. Phys. Chem.* **1986**, *90*, 1954. (c) Hart, E. J.; Henglein, A. *J. Phys. Chem.* **1985**, *89*, 4342.
(12) (a) Kondo, T.; Murali Krishna, C.; Riesz, P. *Radiat. Res.* **1989**, *118*, 211. (b) Gutierrez, M.; Henglein, A.; Fischer, Ch.-H. *Int. J. Radiat. Biol.* **1986**, *50*, 313.
(13) (a) Murali Krishna, C.; Kondo, T.; Riesz, P. *Radiat. Phys. Chem.* **1988**, *32*, 121. (b) Kondo, T.; Murali Krishna, C.; Riesz, P. *Int. J. Radiat. Biol.* **1988**, *53*, 891.
(14) (a) Alegria, A. E.; Lion, Y.; Kondo, T.; Riesz, P. *J. Phys. Chem.* **1989**, *93*, 490. (b) Gutierrez, M.; Henglein, A. *J. Phys. Chem.* **1988**, *92*, 2978.

0022-3654/91/2095-3630$02.50/0

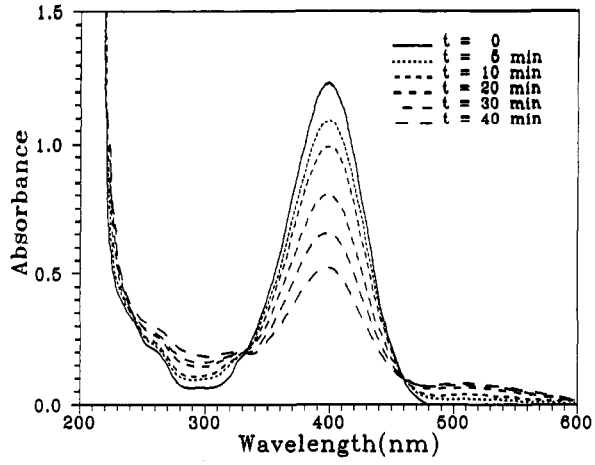

Figure 1. Absorption spectra evolution with sonication time.

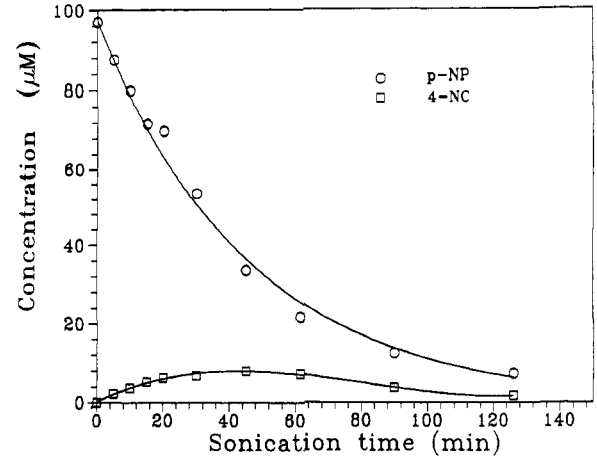

Figure 2. PNP and 4-NC concentrations versus sonication time at pH 5.

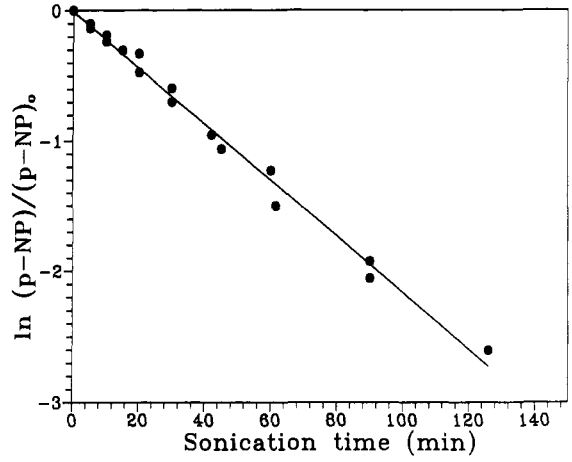

Figure 3. First-order plot of PNP decay at pH 5.

inants found in water.

Experimental Section

The ultrasonic irradiation of aqueous solutions of PNP was carried out with a Branson 200 sonifier that was operated at 20 kHz and with an output of electrical power to converter equal to 84 W. Reactions were performed in a stainless-steel continuous-flow reaction cell operated in the batch mode (Sonics & Materials). The reactor was encased in a self-contained water jacket and was cooled with water to 15 °C. The measured reaction temperature inside the cell was 30 °C. All reactions were carried out with air-saturated solutions. Two openings on the upper part of the reactor allowed for a continuous exposure to air during the course of sonication. Unless otherwise stated experiments were performed with aqueous solutions adjusted to an initial pH of 5.

Quantification of PNP and 4-nitrocatechol (4-NC) was achieved by the measurement of the their respective absorbancies in alkaline solution (0.1 M NaOH) at λ = 401 nm (ϵ = 19 200 M^{-1} cm^{-1} for PNP) and 512 nm (ϵ = 12 300 M^{-1} cm^{-1} for 4-NC).[15] The measured absorbance of PNP was corrected for the small contributions due to 4-NC at 401 nm (ϵ = 6500 M^{-1} cm^{-1}).[15] The concentration of *p*-benzoquinone (*p*-BQ) was determined spectrophotometrically in a solution containing 20% *n*-butylamine at λ = 345 nm.[16] The measured absorbance at 345 nm was corrected for the contributions due to PNP and 4-NC (extinction coefficients in 20% *n*-butylamine: *p*-BQ, ϵ_{345} = 26 400 M^{-1} cm^{-1}; *p*-NP, ϵ_{345} = 3800 M^{-1} cm^{-1}; 4-NC, ϵ_{345} = 3300 M^{-1} cm^{-1}).

Nitrite, nitrate, formate, and oxalate were determined with a Dionex 2020i ion chromatograph and a Dionex AS4-A column. The IC eluents were 2.2 mM CO_3^{2-}, 2.8 mM HCO_3^-, and 5 mM $B_4O_7^{2-}$. The concentration of H^+ was determined with a Radiometer autotitration system. Ionic strength was adjusted after sonication to 1 mM with Na_2SO_4. Hydrogen peroxide was determined iodometrically and fluorometrically as described previously.[17] Kinetic runs were carried out by sonication of a sample for a desired length of time. At that time an aliquot was withdrawn for complete chemical analysis. Kinetic experiments were continued after cleaning the cell thoroughly and filling it with fresh solution. Before analysis all samples were filterd with 0.2-μm HPLC filters (from Gelman) to remove Ti particles produced during sonication by erosion of the Ti tip of the sonication horn. Loss of PNP or its degradation products by adsorption to the HPLC filters was not observed. The water employed in all preparations was purified by a Milli-Q/RO system (18 Mohm resistivity) produced by Millipore. Absorption spectra were measured with a Shimadzu MPS-2000 UV–vis spectrophotometer and fluorescence analyses were performed with a Shimadzu RF-540 spectrofluorimeter.

(15) Kortum, G. *Z. Phys. Chem.* [*B*] **1939**, *42*, 39.
(16) Lacoste, R. J.; Covington, J. R.; Frisone, G. *Anal. Chem.* **1960**, *32*, 990.
(17) Kormann, C.; Bahnemann, D. W.; Hoffmann, M. R. *Environ. Sci. Technol.* **1988**, *22*, 798.

Results

Exposure of 25-mL solutions of 100 μM *p*-NP to ultrasound in the presence of air resulted in a decrease in the absorption due to PNP at 401 nm and the subsequent formation of an new absorption band at 512 nm corresponding to 4-NC. The evolution of the absorption spectra with time is presented in Figure 1. Two near (but not exact) isosbestic points were observed at ~460 and ~335 nm. At sonication times longer than 40 min these apparent isosbestic points were lost. Figure 2 shows the concentration vs irradiation time profiles for PNP and 4-NC. The initial increase in the [4-NC] was linear with time. A maximum concentration of 4-NC was observed after 40 min of sonication. The concentration of PNP decreased exponentially with sonication time.

Figure 3 shows a first-order plot of ln [PNP] vs time. The ultrasonic degradation of PNP followed apparent first-order kinetics for at least four half-lives. A first-order rate constant of $k_1 = 3.7 \times 10^{-4}$ s^{-1} was determined from the slope of this plot.

Nitrite and nitrate were found as primary nitrogen-containing products of the degradation of PNP. The time-dependent variations in the concentrations of these ions are shown in Figure 4a. NO_2^- appears to be the main product at short sonication times; it reached a maximum concentration of 57 μM after 42 min of sonication. The concentration of NO_3^- increased continuously with time. The results of Figure 4a were obtained by analyzing the samples immediately after sonication. However, if the IC analysis were repeated on the same sample aliquot after several hours, NO_3^- was found as the main product and only traces (~6 μM) of nitrite were detected. These results suggest that NO_2^- is the principal product of the decay of PNP by ultrasound.

It is well-known that nitrite and nitrate are generated by the ultrasonic oxidation of N_2 in air-saturated aqueous solutions.[1] Sonication of pure water under the same experimental conditions used for the PNP solutions produced substantial concentrations

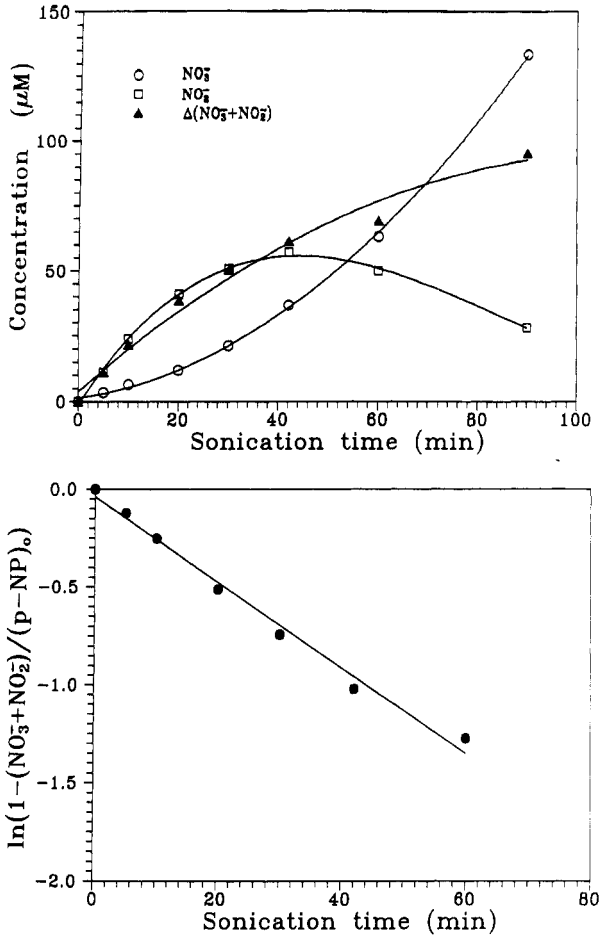

Figure 4. (a, top) NO_2^- and NO_3^- formation during sonication. (b, bottom) First-order plot of NO_x^- formation at pH 5.

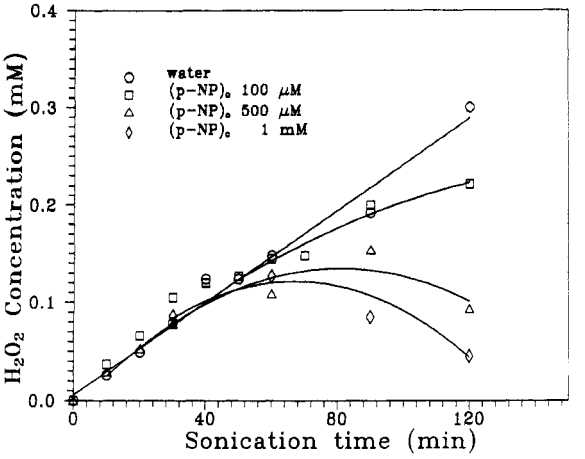

Figure 5. Hydrogen peroxide generation during sonication.

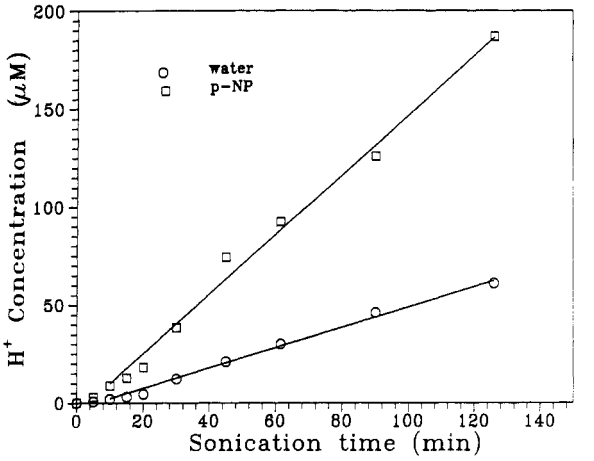

Figure 6. $[H^+]$ increase during sonication.

of these ions. The determination of the $[NO_3^-] + [NO_2^-]$ produced by the decay of PNP was possible by subtracting $[NO_3^-] + [NO_2^-]$ produced in the control reaction with purified water from the sum of the concentrations of these ions in the PNP solutions, for each irradiation time as follows

$$([NO_3^-]^t_{PNP} + [NO_2^-]^t_{PNP}) - ([NO_3^-]^t_{H_2O} + [NO_2^-]^t_{H_2O}) = (NO_3^- + NO_2^-) \quad (I)$$

where $[NO_x^-]^t_{PNP}$ represents the amount of NO_x^- produced by sonication of PNP solutions and $[NO_x^-]^t_{H_2O}$ represents the amount of NO_x^- formed by sonication of water at time t. The results of this calculation are included in Figure 4a. From these results we see that NO_x^- (i.e., $NO_3^- + NO_2^-$) increased exponentially with irradiation time between 0 and 60 min. The corresponding first-order plot of these results is shown in Figure 4b. A first-order rate constant for the formation of $(NO_2^- + NO_3^-)$ of $k_1 = 4 \times 10^{-4}$ s^{-1} was obtained from this data (Figure 4b).

As shown in Figure 5, H_2O_2 was produced during the decay of PNP by sonication. These results were obtained by analyzing the PNP solutions immediately after sonication. Lower peroxide concentrations were detected when irradiated samples were left in the dark for several hours and then reanalyzed. The decrease of $[H_2O_2]$ during the postirradiation period can be attributed to the reaction of H_2O_2 with NO_2^- to yield NO_3^-.[20] No organic peroxides were detected with the iodide-difference method of Kormann et al.[17] Both analytical methods for H_2O_2 gave identical results. Henglein[1] has shown that H_2O_2 is generated by the action of ultrasonic waves on pure water. Under our experimental conditions sonolysis of the solvent alone led to a linear increase of $[H_2O_2]$ vs irradiation time with a rate constant of 4×10^{-8} M s^{-1}. Sonication of solutions containing PNP yielded initially the same result as shown in Figure 5. At longer irradiation times the observed concentrations of H_2O_2 were lower in PNP solutions than in pure water. The deviation from the results obtained with water alone increased with increasing initial concentrations of PNP. Also, this deviation occurred at earlier stages of the reaction in solutions containing high concentrations of nitrophenol. However, the initial rate of formation of H_2O_2 was the same as in pure water alone, regardless of the [PNP].

Hydrogen ions were formed by the action of ultrasound on a 100 μM PNP solution. Figure 6 shows the increase of proton concentrations in a PNP solution and in pure water as a function of sonication time. The increase of $[H^+]$ was initially slow in both systems. However, after 10 min of irradiation, $[H^+]$ increased. The sonolysis of pure water produced a linear increase of $[H^+]$ as a function of time with an apparent zero-order rate constant of 8.3×10^{-9} M min^{-1}. At sonication times ≥20 min, $[NO_2^-] + [NO_3^-]/[H^+] = 1$. On the other hand, in sonicated PNP solutions the increase of $[H^+]$ (at $t \geq 10$ min) appeared to be first order with an apparent first-order rate constant of $k_1 = 3 \times 10^{-4}$ s^{-1} after correction of the $[H^+]$ in manner analogous to the correction made for $NO_3^- + NO_2^-$ (see eq I).

Since the rate of production of H^+ was less than the rate of generation of NO_3^- and NO_2^- in PNP solutions, a pH-buffering effect by some of the products was indicated. IC analyses of the sonicated PNP solutions showed clearly that HCO_2^- and $C_2O_4^{2-}$ were formed as a function of time (Figure 7). The $[HCO_2^-]$ increased linearly with sonication time with an apparent zero-order rate constant of 4.2×10^{-9} M s^{-1}. After an induction period of ~10 min, oxalate was produced with an apparent zero-order rate constant of 5×10^{-9} M s^{-1}.

p-Benzoquinone (*p*-BQ) was also formed upon exposure of PNP solutions to ultrasound. The [*p*-BQ] vs sonication time profile is shown in Figure 8. Concentrations of *p*-BQ increased during the first 30 min of sonication to about 17 μM and remained nearly constant at longer reaction times. It should be noted that the *n*-butylamine method responds to *p*-BQ. However, hydroquinone is oxidized rapidly in air to *p*-BQ in alkaline *n*-butylamine solu-

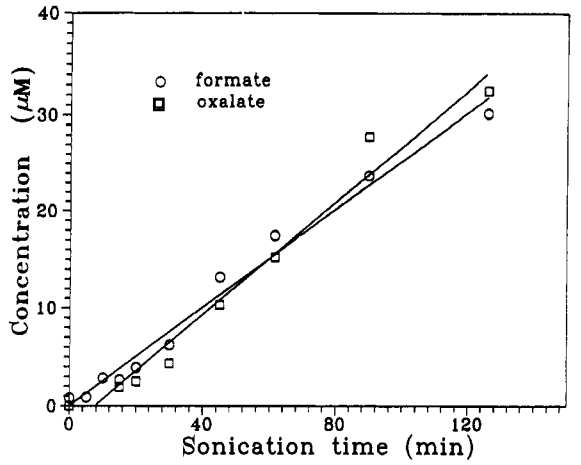

Figure 7. Formate and oxalate formation during sonication.

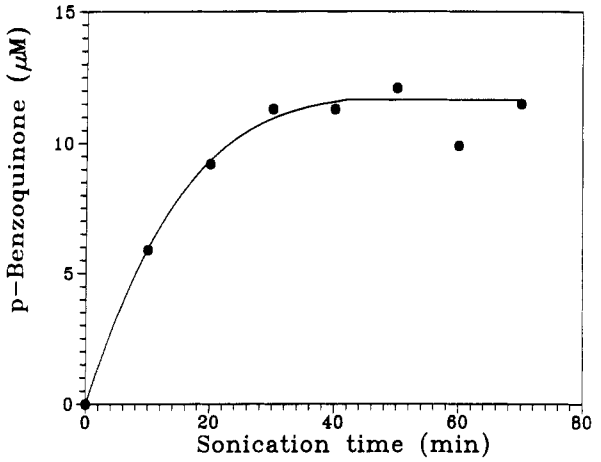

Figure 8. *p*-BQ concentration versus sonication time at pH 5, $[PNP]_0$ = 100 μM.

tions.[16] Hence, the results depicted in Figure 8 correspond to summation of *p*-BQ and hydroquinone.

As mentioned above, PNP decayed in the presence of ultrasound via apparent first-order kinetics. However, the rate of PNP decay by sonication was found to be dependent on the initial concentration of PNP ($[PNP]_i$) as shown in Figure 9a. While PNP decayed exponentially with time irrespective of the PNP concentration, the apparent first-order rate constant decreased from 1.37×10^{-2} s^{-1} at $[PNP]_i$ = 10 μM to 6.17×10^{-5} s^{-1} at $[PNP]_i$ = 1 mM. A plot of log k_1 vs log $[PNP]_i$ yielded a straight-line (r^2 = 0.99) relationship from which the following empirical equation, $k_1 = 3.83 \times 10^{-7}[PNP]_i^{-0.7}$, was obtained.

The formation of 4-NC from PNP followed zero-order kinetics at short sonication times (Figure 2, $[PNP]_i$ = 100 μM) with an apparent rate constant of $k_0 = 6.17 \times 10^{-9}$ M s^{-1}. However, the rate of formation increased with increasing $[PNP]_i$. These results are illustrated in Figure 9b. The initial zero-order rate constant varied from $k_0 = 3.0 \times 10^{-9}$ M s^{-1} at $[PNP]_i$ = 10 μM to k_0 = 1.7×10^{-8} M s^{-1} at $[PNP]_i$ = 1 mM.

Changes in the initial pH (pH_i) of the PNP solutions also affected the decay of PNP as shown in Figure 10. PNP decayed exponentially with time at all pH values. The apparent first-order rate constant decreased from $k_1 = 3.67 \times 10^{-4}$ s^{-1} at pH_i = 5 to $k_1 = 2.0 \times 10^{-4}$ s^{-1} at pH_0 = 8 and remained constant up to pH_0 = 10.

At $pH_0 > 10$ the apparent first-order rate constant increased slightly because of the slow thermal reaction between PNP and the products of the base-catalyzed decomposition of H_2O_2. This thermal reaction was detected as a postirradiation decay of PNP in alkaline solutions, which extended for several hours. The postirradiation effect was detected in all sonicated PNP solutions that were made alkaline for the analysis of the nitrophenoxide ion at 401 nm. No postirradiation decay of PNP was observed

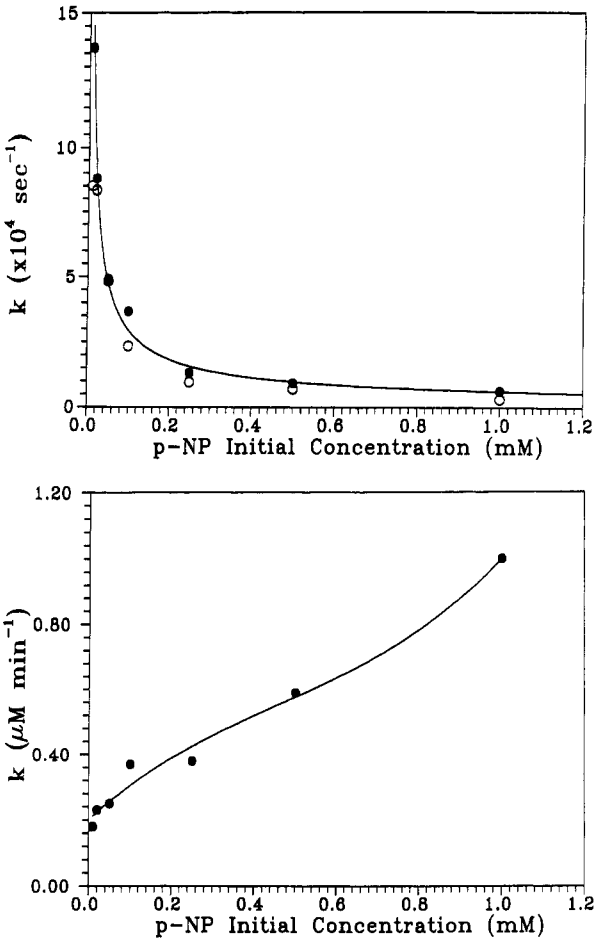

Figure 9. (a, top) Effect of $[PNP]_0$ on the rate of PNP degradation. (b, bottom) Effect of $[PNP]_0$ on the initial rate of 4-NC formation.

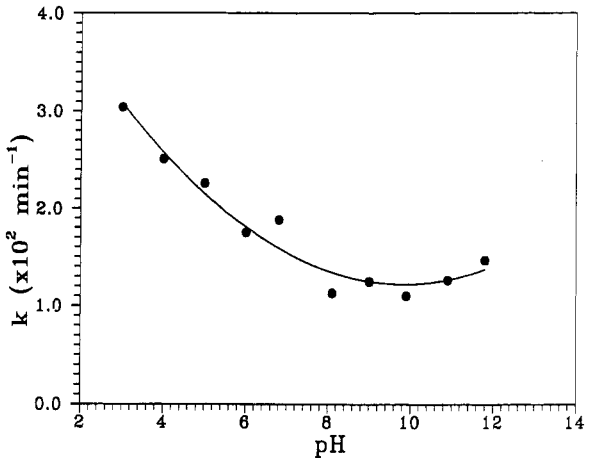

Figure 10. Effect of pH on the rate of PNP degradation.

in solutions that were acidified to pH = 1 immediately after sonication. The latter solutions were analyzed spectrophotometrically for PNP at λ = 317 nm (ε = 10190 M^{-1} cm^{-1}). In the experiments at high pH, only borax and phosphate buffers were used. This procedure was adopted to avoid possible interference from the buffers due to the scavenging of H• and •OH radicals. Similar results were obtained when experiments carried out in the presence of phosphate buffers were repeated with borax buffers.

A modest increase of k_1 was noticed when the pH was lowered with H_2SO_4 from pH = 5 to pH = 4 (Figure 10). At pH < 4 the apparent first-order rate constant increased to 5.0×10^{-4} s^{-1} (pH = 3). However, at $[H^+] > 1$ mM results were not reproducible. The increase of k_1 with increasing acid concentrations cannot be explained by ionic strength effects, since sonication of

PNP solutions at pH = 5 in the presence of 0.5 mM Na_2SO_4 or 1 mM $NaNO_3$ gave identical results with those obtained in the absence of these electrolytes.

4-NC was formed with an apparent zero-order rate of $k_0 = 6.17 \times 10^{-9}$ M s^{-1} which was found to be independent of pH over pH range of 4–10. At pH = 3 the rate of formation decreased to $k_0 = 1.67 \times 10^{-9}$ M s^{-1}. A similar effect was noticed in alkaline solutions where $k_0 = 1 \times 10^{-9}$ M s^{-1} at pH = 10.9 and $k_0 = 6.67 \times 10^{-10}$ M s^{-1} at pH = 11.8.

Several experiments were performed in order to evaluate the sonochemical reactivity of some of the reaction products and their influence in the reactions of PNP. For this purpose, air-saturated solutions containing 20 μM 4-NC were exposed to ultrasound. The concentration of 4-NC decreased exponentially with time with an apparent first-order rate constant of $k' = 9.83 \times 10^{-4}$ s^{-1}. This result is very close to the rate constant obtained in a solution containing 20 μM PNP ($k_1 = 8.83 \times 10^{-4}$ s^{-1}). Sonication of a mixture containing 100 μM PNP and 20 μM 4-NC resulted in an apparent first-order rate constant for the decay of PNP equal to $k_1 = 2.5 \times 10^{-4}$ s^{-1}. The concentration of 4-NC decreased continuously with sonication time. Under these conditions the decay of 4-NC was faster at all sonication times than its formation from PNP. However, 4-NC decayed in the presence of 100 μM PNP with an apparent first-order rate constant of 2.83×10^{-5} s^{-1}, a value significantly lower than that obtained in the absence of PNP.

While NO_3^- did not interfere with the sonochemical reactions of PNP, NO_2^- appeared to affect the decay of *p*-nitrophenol. Irradiation of a solution containing 100 μM PNP and 100 μM $NaNO_2$ with ultrasound resulted in a slower disappearance of PNP ($k_1 = 2.0 \times 10^{-4}$ s^{-1}) when compared to a kinetic run in the absence of NO_2^- ($k_1 = 3.67 \times 10^{-4}$ s^{-1}). In addition, we found that the formation of 4-NC was slower in the presence of NO_2^-. The apparent zero-order rate constant for the formation of nitrocatechol was about one half ($k_0 = 3.0 \times 10^{-9}$ M s^{-1}) of the rate constant obtained in the absence of NO_2^- ions ($k_0 = 6.2 \times 10^{-9}$ M s^{-1}).

On several occasions the spectrophotometric determination of PNP at 401 nm in alkaline solutions was verified by measurements of [PNP] in acid solution at 317 nm ($\epsilon = 10\,200$ M^{-1} cm^{-1}). Excellent agreement (deviation < 5%) between the two methods was obtained after the absorption at 317 nm was corrected for the small contributions of 4-NC ($\epsilon = 5700$ M^{-1} cm^{-1}). No absorption at $\lambda = 348$ nm was detected in PNP solutions acidified to pH = 1 after sonication. Knowing that in acid solution neither PNP nor 4-NC absorbs at this wavelength and that the absorption of 4-nitroresorcinol at low pH is strongest at $\lambda = 348$ nm ($\epsilon = 8850$ M^{-1} cm^{-1}),[18] it can be concluded that the concentration of nitroresorcinol was less than 5 μM at all sonication times. Products of the nitration of PNP such as 2,4-dinitrophenol were not detected in concentrations above the limit of detection of 7 μM.

The rate of disappearance of PNP was found to be independent of the volume of sonicated solution (20–40 mL). Sonication of air-saturated solutions, which were not exposed to air during the course of sonication, produced the same results as those obtained with air-equilibrated solutions. Furthermore, identical results were obtained by using continuous sonication or pulsed sonication (0.5 s sonication per every second). The comparison was made using the net sonication times in the case of pulse experiments. No significant effects due to tip erosion were found.

Discussion

We have shown clearly that the action of ultrasound on PNP in aqueous solutions resulted in its degradation with the formation of NO_2^-, NO_3^-, and H^+ as primary products and with HCO_2^-, $C_2O_4^{2-}$, 4-NC, and H_2O_2 as secondary products. Several reaction mechanisms can be postulated to account for these observations.

SCHEME I

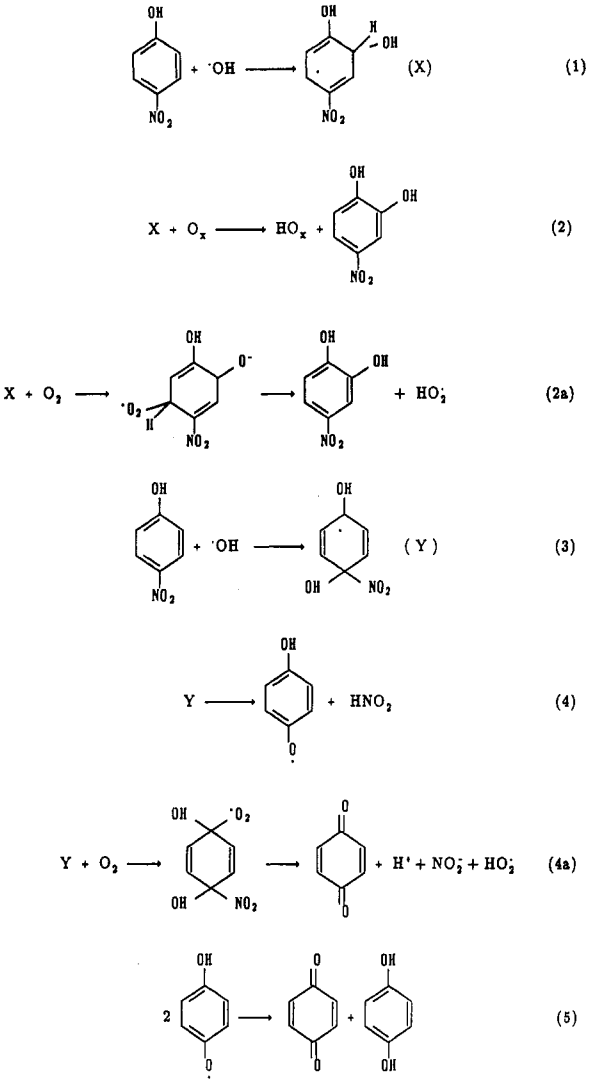

Since PNP boils at $T \geq 166$ °C,[21] high-temperature reactions of PNP vapor inside the cavitating bubbles can be discounted due to its low vapor pressure. Processes leading to the denitrification of PNP are more likely to occur in the hot solvent layer surrounding the gas bubbles or in the bulk of the solution. A degradation mechanism that involves •OH radical attack on PNP appears plausible.[22] Results of radiation-chemistry investigations have shown that •OH reacts rapidly with PNP to produce 4-NC, *p*-BQ, and NO_2^-.[23-25] A plausible mechanism for the reaction of hydroxyl radicals with PNP is shown in Scheme I: where O_x in eq 2 is an oxidant and HO_x is the reduced form of O_x. Both radicals X and Y have been identified by ESR as the major products of •OH attack on PNP.[26] The unknown oxidant O_x could be the benzoquinone radical produced by eq 4 or products from the attack of •OH in positions ortho (at the carbon atom of the ring bonded to the hydroxyl function) or meta. At pH = 5, about 15% of the •OH radicals attack PNP via eqs 1b through 5 to produce NO_2^-, whereas 70% of •OH radicals react with

(18) (a) Sunkel, J.; Staude, H. *Ber. Bunsen-Ges. Phys. Chem.* **1969**, *73*, 203. (b) Sunkel, J.; Staude, H. *Ber. Bunsen-Ges. Phys. Chem.* **1968**, *72*, 567.
(19) Mead, E. L.; Sutherland, R. G.; Verral, R. *Can. J. Chem.* **1976**, *54*, 1114.
(20) Bhattacharyya, P. K.; Veeraghavan, R. *Int. J. Chem. Kinet.* **1977**, *9*, 629.
(21) Deason, W. R.; Koerner, W. E.; Munch, R. H. *Ind. Eng. Chem.* **1959**, *51*, 1001.
(22) Buxton, G. V.; Greestock, C. L.; Helman, W. P.; Ross, A. B. *J. Phys. Chem. Ref. Data* **1988**, *17*, 513.
(23) (a) O'Neil, P.; Steenken, S.; Van Der Linde, H.; Schulte-Frohlinde, D. *Radiat. Phys. Chem.* **1978**, *12*, 13. (b) Volkert, O.; Termens, G.; Schulte-Frohlinde, D. *Z. Phys. Chem. Munich* **1967**, *56*, 261. (c) Grasslin, D.; Merger, F.; Schulte-Frohlinde, D.; Volkert, O. *Z. Phys. Chem. Munich* **1966**, *51*, 84.
(24) Suarez, C.; Louys, F.; Gunter, K.; Eiben, K. *Tetrahedron Lett.* **1970**, 575.
(25) Cercek, B.; Ebert, M. *Adv. Chem. Ser.* **1968**, *81*, 210.
(26) Eiben, K.; Schulte-Frohlinde, D.; Suarez, C.; Zorn, D. *Int. J. Radiat. Phys. Chem.* **1971**, *3*, 409.

formation of 4-NC according to eqs 1a–3.[23a,24] The ratio of yields for the products is *p*-BQ (+ hydroquinone):NO_2^-:4-NC = 1:1:4.7. At pH ≥ 8, however, 30% of the hydroxyl radicals react to produce nitrite and 5% of the •OH radicals reacts with PNP to form 4-NC.[23a,24] Under these conditions, the ratio of yields for the different products is *p*-Bq (+ hydroquinone):NO_2^-:4-NC = 1:1:1.8.

In aerated solutions the products, X and Y, react with oxygen ($k = 1.7 \times 10^6$ M^{-1} s^{-1} [25]) via eqs 2a and 4a to yield the same products (and ratio of products) produced by eqs 1–5 with the exception of hydroquinone. Instead, only *p*-BQ is produced, which is equivalent to the oxidation of hydroquinone by O_2 to produce hydrogen peroxide. In aerated solutions, the peroxy radicals formed by eqs 2a and 4a will decay with generation of H_2O_2:[27]

$$2HO_2^{\bullet} \rightarrow H_2O_2 + O_2 \qquad (6)$$

For every pair of •OH radicals which react with PNP one molecule of H_2O_2 is produced. This means that, in PNP solutions, the same amounts of peroxide are produced from hydroxyl radical reactions as by sonolysis of pure water. In the absence of PNP, •OH recombines to form hydrogen peroxide:[22]

$$2^{\bullet}OH \rightarrow H_2O_2 \qquad (7)$$

Hydrogen atoms are known to react with PNP but the rate constant of this reaction has not been measured.[25] •OH and •H will react preferentially with scavengers present in the cavition bubbles. The main scavenger for H atoms in the gas phase of the bubbles is oxygen. The reaction between H and O_2 at high temperatures is believed to produce oxygen atoms and OH radicals:[11b]

$$H + O_2 \rightarrow {}^{\bullet}OH + {}^{\bullet}O \qquad (8)$$

According to this reaction, hydrogen atoms are converted to hydroxyl radicals and oxygen atoms before they can reach the solution and react with PNP. Oxygen atoms and hydroxyl radicals are expected to be partially scavenged by nitrogen in the gas bubbles.[11a] These reactions lead to the formation of NO_2^- and NO_3^- in the sonolysis of air-saturated water. Only those radicals which escape into solution without reacting with N_2 will be scavenged by PNP. This argument implies that nitrate and nitrite are produced by two independent mechanisms during the sonolysis of PNP solutions: (a) via the same gas-phase reaction which takes place in pure water and (b) from the decay of PNP molecules. The basic assumption that PNP did not interfere with the gas-phase chemistry taking place inside the hot cavities is confirmed by the close agreement of k_1 calculated from the decay of PNP and the rate constants derived from the formation of NO_2^- and NO_3^- as well as from the H^+ results.

However, a closer inspection of the results reveals that the sonochemical decay of PNP in aqueous solution cannot be explained only on the basis of reactions between •OH and PNP in the bulk solution phase. For example, PNP decreased exponentially with sonication time, while PNP attack by •OH in homogeneous solution follows zero-order kinetics.[24,25] First-order kinetics have been observed in the sonication of thymine[2] and phenol.[28] In both cases the concentration decreased exponentially with time at initial concentrations of substrate ≤1 mM, whereas at higher concentrations the reactions followed zero-order kinetics.[2,28] These results have been explained by assuming that thymine and phenol react preferentially in the interfacial region with free radicals.[2] At low substrate concentrations (≤1 mM) the rate-limiting step was considered to be the diffusion of substrate to the reaction zone, while the reaction of free radicals and substrate was assumed to occur very fast (diffusion controlled.)[2] At high solute concentrations (>1 mM) the reactive radicals will be scavenged as they reach the interface; thus zero-order kinetics are observed.[2] This model is only correct if the radical concentrations at the interface are very high, otherwise low concentrations of solute would be sufficient to scavenge most of the free radicals.

However, this model presents a simplified version of the events that occur during sonolysis. For example, solute–radical reactions in the bulk solution[11a–13] are not considered. Also, no allowance is made for thermal decomposition reactions of the solute in cavities as well as reactions in the hot surroundings of the cavities.

It is, therefore, not surprising that several observations made in sonolysis experiments with PNP solutions remained unexplained. The unexplained results are as follows:

1. According to the above model, the first-order decay of substrate is related to diffusion of substrate to the reaction zone. In the case of PNP this assumption implies that diffusion of the PNP molecules to the interface was highest at the lowest [PNP], since k_1 increased with decreasing concentration of the substrate (Figure 9a). Obviously, such a conclusion is not correct.

2. If *p*-BQ is formed exclusively via the sequence of eqs 3 and 4a the measured concentrations of quinone represent only 13% of the products produced by reaction of •OH with PNP. We observed that after 10 min of sonication [*p*-BQ] = 5.9 μM. The free-radical model predicts a change of [PNP] equal to Δ[PNP] = 45 μM for the same reaction time. The predicted value of Δ[PNP] does not agree with the experimental value of 17 μM.

3. The initial ratio of products from the sonolysis of PNP was *p*-BQ:NO_2^-:4-NC = 1:3.6:0.7. In contrast, the observed products of •OH attack on PNP were formed initially with a ratio of *p*-BQ:NO_2^-:4-NC of 1:1:4.7.[23a,24] Note that in the case of phenol the ratio of products, at short reaction times, was the same at high[29] as well as at low[30] •OH concentrations. By analogy, the initial ratio of products from hydroxyl radical attack on PNP is not expected to vary with changing [•OH]. The differences in the ratio of products suggest that the mechanism of reaction in the sonolysis of PNP is different from the mechanism represented by reactions 1–5. It might be argued that the different ratio of products in the sonolysis reflects a different selectivity of the •OH attack at high temperatures. However, extensive investigations on high-temperature reactions of •OH with aromatic compounds have demonstrated that at $T \geq 400$ K the main reaction pathway is hydrogen atom abstraction instead of addition to the aromatic ring.[31] Thus, the denitrification of PNP initiated by reaction 1 is not expected to be the main reaction pathway in the high-temperature regions of the interface.

The relatively fast decay of PNP can be explained by the thermal decomposition of PNP in the near vicinity region of the hot collapsing gas cavities. The thermal instability of nitroaromatic compounds, which forms the basis for their use as explosives, is well documented.[21,32,33] As mentioned above, PNP is known to decay thermally at $T \geq 166$ °C (439 K). While no kinetic information is available for PNP, closely related compounds such as nitrobenzene (NB) and *p*-nitrotoluene (*p*-NT) have been recently studied by shock-tube experiments.[33] Both compounds are decomposed at high temperatures by cleavage of the C–NO_2 bond. The analogous reactions for PNP are

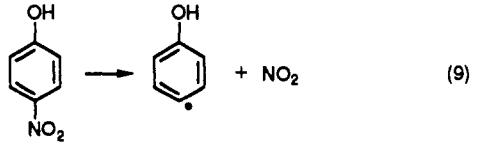

(9)

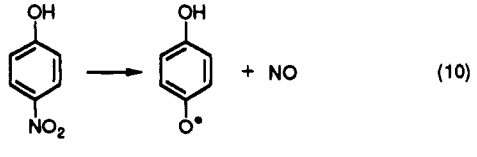

(10)

(27) Bielski, H. J.; Cabelli, D. E.; Arudi, R. L.; Ross, A. B. *J. Phys. Chem. Ref. Data* **1985**, *14*, 1041.

(28) (a) Chen, J. W.; Chang, J. A.; Smith, G. V. *Chem. Eng. Prog. Symp. Ser.* **1971**, *67*, 18. (b) Lure, Yu. Yu.; Kandzas, P. F.; Mokina, A. A. *Russ. J. Phys. Chem.* **1962**, *36*, 1422.

(29) Hashimoto, S.; Miyata, T.; Washino, M.; Kawakami, W. *Environ. Sci. Technol.* **1979**, *13*, 71.

(30) Raghavan, N. V.; Steenken, S. *J. Am. Chem. Soc.* **1980**, *102*, 3495.

(31) (a) He, Y. Z.; Mallard, W. G.; Tsang, W. *J. Phys. Chem.* **1988**, *92*, 2196. (b) Atkinson, R. *Chem. Rev.* **1985**, *85*, 69.

(32) Maksimov, Yu. Ya. *Russ. J. Phys. Chem.* **1972**, *46*, 990.

(33) Tsang, W.; Robaugh, D.; Mallard, W. G. *J. Phys. Chem.* **1986**, *90*, 5968.

Assuming that NO and NO_2 are the precursors of NO_2^- (vide infra), the unimolecular decay of PNP via eqs 9 and 10 provides a plausible explanation for the observed first-order denitrification of PNP by the action of ultrasound. In order to understand the formation of 4-NC it has to be assumed that PNP decays by parallel zero- and first-order processes:

$$-d[PNP]/dt = k_0' + k_1[PNP]_t \qquad (11)$$

There k_1 represents $k_9 + k_{10}$ and k_0' is the zero-order rate constant for the reaction between •OH and PNP, which produces mainly 4-NC. The solution to eq 11 is

$$[PNP]_t = \frac{-k_0'}{k_1} + \left(\frac{-k_0'}{k_1} + [PNP]_0\right)e^{-k_1 t} \qquad (12)$$

Since approximately 70% of the •OH radicals that react with PNP yield 4-NC, the value of $k_0' \simeq k_0/0.7$. Given the experimental values of k_0 shown in Figure 9b, the values of k_0' for different initial concentrations of PNP can be estimated. By use of these results and the measured concentrations of PNP at different sonication times, the apparent first-order rate constants at different concentrations of PNP were calculated by using a nonlinear fitting procedure and are presented in curve 2 of Figure 9a. The calculated values of k_1 agree closely with the experimental values for k_1. Only kinetic data obtained at short sonication times (i.e., at low fractions of PNP destroyed ($1\text{-}F \leq 20\%$)) were used for this analysis. It can be concluded that the exponential decay of [PNP] via eqs 9 and 10 is the dominant process and that •OH radical reactions contribute to PNP decay only at short reaction times. If this interpretation is correct, 4-NC is formed via a zero-order process represented by reactions 1 and 2a and decays exponentially with time via reactions analogous to eqs 9 and 10.

The present model can also account for the unusually high ratio of *p*-BQ to 4-NC of 1:0.7 observed from sonolysis compared to the ratio obtained from radiolysis of PNP (i.e., *p*-BQ:4-NC = 0.19:1).[23a,24] Tsang et al.[33] identified two different reaction channels for the pyrolysis of NB and *p*-NT; they were identified as (1) the direct loss of NO_2 and (2) the isomerization of bound NO_2 followed by elimination of NO. In our case these two reaction pathways are represented by eqs 9 and 10, respectively. For NB and *p*-NT Tsang et al. estimated that the ratio of rate constants are $k_{elimination}:k_{isomerization} = 2:1$. Hence, the fraction of products formed by the isomerization channel is simply $k_{isomerization}/(k_{elimination} + k_{isomerization}) = 1/3$. Assuming a similar mechanism in our case, it appears that a reaction path involving first eq 9 followed by eq 5 contributed to the formation of *p*-BQ. From the pyrolysis mechanism it is predicted that $[p\text{-BQ}](\Delta[PNP])^{-1} = 1/3$ provided that the decay of *p*-BQ is negligible. After both [*p*-BQ] and Δ[PNP] are corrected for the contributions from the •OH radical reactions, the experimental ratio is 1/2.2 (at $t = 10$ min). The difference between the expected ratio and the experimental value can be explained by assuming that a fraction of the NO_2• reacted with the aromatic hydroxy radical generated via eqs 9 and 13 followed by reaction 5.

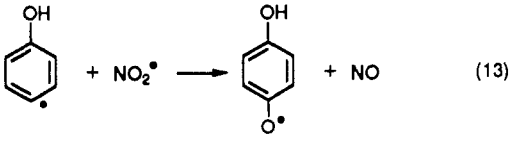

(13)

Reaction 13 is analogous to the postulated mechanism for the attack of NO_2• on hydroxycyclohexadienyl radicals.[34] Thus, according to our model, *p*-BQ is produced mainly by pyrolysis of PNP while the formation of *p*-BQ by •OH radical attack is of minor importance.

The proposed mechanism for the decomposition of PNP based on pyrolysis reactions not only explains our kinetic observations but enables us to estimate the reaction temperatures in the interfacial region. With the known rate expressions for model compounds and assuming a similar rate expression for the case of PNP, the average temperature in the reaction zone can be evaluated. This method, which is called chemical thermometry, has been used previously to estimate the temperature inside and in the surroundings of collapsing bubbles in hydrocarbon solvents.[4] From the values of k_1 shown in Figure 9a and using $k(C_6H_5NO_2 \rightarrow C_6H_5^\bullet + NO_2^\bullet) = 1.9 \times 10^{15}e^{-3306/T}\ s^{-1}$,[33] the temperature of the interfacial region was found to vary between $T = 740$ and 790 K (see Table I). The same results were obtained by using the rate expression for *p*-NT.[33] Higher temperatures (~2000 K) were estimated for the interface of bubbles in hydrocarbon solvents.[4] The difference in temperature between water and hydrocarbons can be explained by considering the different thermal conductivities of each solvent. Because of the higher thermal conductivity of H_2O, heat will move faster in this solvent and the peak interfacial temperature is expected to be lower.[35] The results presented in Table I are considered to be lower limits for the average temperature in the interfacial region, since k_1 is only an apparent first-order rate constant for the reaction.

TABLE I: Calculated First-Order PNP Thermal Decomposition Rates and Corresponding Effective Temperatures of the Reaction Zone

[*p*-NP], μM	10^4k, s^{-1}	T,[a] K	[*p*-NP], μM	10^4k, s^{-1}	T,[a] K
10	8.50	782	250	0.96	743
20	8.33	781	500	0.70	738
50	4.83	771	1000	0.30	724
100	2.33	758			

[a] Calculated assuming $k_1 = 1.9 \times 10^{15}e^{-33026/T}$.

In order to explain the chemical processes, which take place at the interface, it is necessary to understand, at least qualitatively, the sequence of events occurring in that region. The local temperature in the solvent surrounding the bubble will be a time-dependent spatial gradient during the collapse of the cavity as proposed earlier for hydrocarbon solvents.[4] Thus, heat will move from the surface of the bubble toward the solution bulk. It is further assumed that •OH generated in the hot bubbles will diffuse to the solvent interface and subsequently through it at a speed similar to that of the front of the heat wave. In the solvent, •OH reacts with PNP. The OH adducts will increase in thermal energy as the temperature of the solvent increases. At the same time PNP molecules situated at the interface having a thermal energy equivalent to or greater than 439 K will react by denitration via eqs 9 and 10. However, this reaction is not restricted to PNP molecules. Addition of OH radicals to the ring of PNP is not expected to increase the strength of the C–NO_2 bond. Therefore, all OH adducts with sufficient thermal energy will undergo denitrification via an analogous mechanism. The threshold temperature for the loss of NO_2 from "OH–PNP" adducts is expected to be similar to the minimum temperature for PNP.

The fate of the resulting OH adducts can be predicted from results gained in high-temperature studies on hydroxyl radicals with aromatics.[31] These studies indicate that at $T \leq 325$ K the addition reaction (eq 14) dominates. For $T \geq 400$ K dissociation

$$^\bullet OH + \text{aromatic} \rightarrow (\text{OH–aromatic}) \qquad (14)$$

of the OH adduct is very fast:

$$(\text{OH–aromatic}) \rightarrow {}^\bullet OH + \text{aromatic} \qquad (15)$$

At $T \simeq 1000$ K hydroxyl radicals and hydrogen atoms react predominantly with phenol via hydrogen atom abstraction from the hydroxy group.[31a] In the case of PNP, the resulting phenoxyl radicals are strong oxidants ($E^\circ = 1.2$ V vs NHE)[36] and will probably re-form PNP after oxidizing other products. The reaction of eq 15 is very interesting because it implies that, after the release of the hydroxyl radical from the aromatic ring, the radical can further diffuse to colder regions of the solvent and react again

(34) Zellner, R.; Fritz, B.; Preidel, M. *Chem. Phys. Lett.* **1985**, *121*, 42.

(35) Weast, R. C., Ed. *CRC Handbook of Chemistry and Physics*, 1st Student ed.; CRC: Boca Raton, FL, 1988; pp E-4, E-10.

(36) Lind, J.; Shew, X.; Eriksen, T. E.; Merenyi, G. *J. Am. Chem. Soc.* **1990**, *112*, 47.

with solute molecules. The temperature dependence of k_{15} has been measured for benzene, bromobenzene, and aniline.[37] For direct comparison with our results with PNP, aniline appears to be the most appropriate since the electron-donating properties of the $-NH_2$ and $-OH$ are similar. Using the corresponding temperature dependence, $k_{15} = 6 \times 10^{11} e^{-8400/T}$ s^{-1},[37] a half-life of 48 ns is calculated for eq 15 at 790 K ($k_{15} = 1.5 \times 10^7$ s^{-1}). This short half-life implies that PNP and probably most of the hydroxylated aromatic products produced by the decay of PNP are relatively nonreactive toward •OH in the high-temperature regions of the interface. This argument leads to the conclusion that formation of 4-NC and denitration of PNP via •OH radical attack (reactions 2a and 4a) occurred in the cooler region of the interface ($T < 439$ K).

Products of eqs 9 and 10 are expected to decay further by pyrolysis and/or free-radical reactions. The preferential formation of nitrite at short sonication times is an indication that the reaction between NO_2 and •OH (eq 16) to form nitric acid is not important. Nitrous acid (i.e., nitrite) is produced via eq 17.[38] Since eq 9

$$NO_2 + {}^{\bullet}OH \rightarrow HNO_3 \quad (16)$$

$$NO + OH \rightarrow HNO_2 \quad (17)$$

is considered to be the main decay pathway for PNP, it appears that NO_2 was rapidly converted to NO presumably by combination of NO_2 with organic radicals produced by pyrolysis reactions in a reaction similar to eq 10:

$$R^{\bullet} + NO_2 \rightarrow RO^{\bullet} + NO \quad (18)$$

While •OH reaction with aromatics followed by O_2 addition can lead to ring opening and formation of polycarboxylic acids,[31b] formation of formate from these acids would require a concerted attack by several hydroxyl radicals. Thus, the generation of formate is consistent with a pyrolysis pathway. Oxalate was detected only after an induction period of about 10 min. Oxalate could be produced by OH radical attack on formate as has been found in the sonolysis of aqueous formate solutions under Ar.[11c] However, the sonolysis of oxygenated formate solutions generates CO_2 and not oxalate.[11c] Reaction of •OH with formic acid at high temperatures also leads to CO_2 in the absence of O_2.[31b] Since at short sonication times only 50% of the degraded PNP is accounted for by the appearance of 4-NC, p-BQ, and HCO_2^-, the remainder could be postulated to be polycarboxylic acids formed as intermediates. The delayed formation of oxalate can be explained if the polycarboxylic acids are formed as precursors.

According to our model PNP was denitrated mainly by pyrolysis reactions but the detected products resulted from pyrolysis and free-radical reactions. The concentration of PNP near the surface of the bubbles, which is the zone of the interface where pyrolysis is expected to take place, is assumed to increase with increasing PNP concentration in solution. However, once the interface is saturated with PNP molecules, no further increase of [PNP] in this region will result upon increasing [PNP] in the solution. It seems that the limiting concentration of PNP at the interface is achieved at $[PNP]_i \simeq 500$ μM, since P (percentage of PNP converted to 4-NC) was nearly independent of concentration in the range $10 \leq [PNP]_i \leq 500$ μM (see Figure 11, Appendix). At $[PNP]_i = 1$ mM the fraction P increased abruptly to 30%, indicating that [PNP] was still increasing in regions far away from the bubble surface. This in turn, allowed PNP to compete successfully with pyrolysis products for •OH. The decrease of k_1 in solutions containing PNP and 4-NC or NO_2^- is explained, in part, assuming that 4-NC and NO_2^- were able to displace some PNP molecules from the interface. In addition, both NO_2^- and 4-NC decay at the interface with formation of NO_2. Nitrite is oxidized by OH radicals to NO_2 according to eq 19.[22] The additional

$$NO_2^-/HNO_2 + {}^{\bullet}OH \rightarrow NO_2 + OH^-/H_2O \quad (19)$$

formation of NO_2 at the interface by reactions other than eq 9 will increase the probability of the reverse reaction (eq −9). This second-order reaction will become faster with increasing $[NO_2]$ resulting in the apparent retardation of PNP decay. The same explanation holds for the results shown in Figure 9a. At low concentrations of PNP only small amounts of NO_2^-, 4-NC, and products from eq 9 are generated by sonication. Thus, the back reverse reaction of eq 9 is expected to be very slow and the unimolecular decay of PNP dominates. As $[PNP]_i$ increased k_1 decreased due to the increasing amounts of products from eq 9 and from the increasing concentrations of NO_2^- and 4-NC, which produced higher $[NO_2]$ and accelerated the reverse of eq 9.

The concentration of PNP in the high-temperature zone of the interface is expected to depend also on solution pH. Evidence gathered in earlier studies suggest that the bubbles are hydrophobic and that hydrophobic compounds can accumulate in the hot surroundings of the interfacial region where they undergo high-temperature reactions. The hydrophobic nature of the aromatic ring should drive PNP molecules to the interfacial zone, whereas the polar NO_2 and OH groups will be repelled from the interface. At pH > pK_a the [PNP] at the interface is expected to be smaller than the concentrations attained at lower pH values, due to the increased repulsion from the interface generated by the phenoxide ion. Furthermore, delocalization of electrons from the deprotonated hydroxyl groups into the aromatic ring will increase the stability of the C–NO_2 bond by increasing the sp^2 character of that bond:

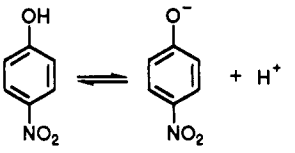

(20)

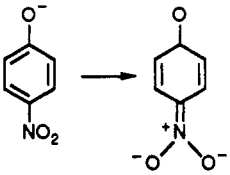

(21)

An increase in the stability of the C–NO_2 bond will lead to an increase in the thermal stability of PNP. The decrease of [PNP] at the interface at pH > 7 (pK_a of PNP = 7.05), together with the increased stability of the nitrophenoxide ion, explains the low values of k_1 found in alkaline solutions. The fact that k_1 is relatively constant between $8 \leq$ pH ≤ 11.8 and is independent of the nature of the buffer (phosphate or borax) provides support for our interpretation.

In conclusion, the application of ultrasound for the control of oxidizable trace contaminants in water has the potential to become a competitive technology with semiconductor photodegradation.[39] For example, the relative efficiency of ultrasound in terms of the total power consumed per mole of p-nitrophenol degraded per liter of water is far superior to photolysis.[39] In our investigation of the ultrasonic oxidation of H_2S, we have found a direct linear relationship between the applied power at a fixed frequency and the observed rate of loss of S(−II). Thus, a continuous-flow stirred-tank (CSTR) probe reactor can attain significant conversion efficiencies at relatively high volumetric flow rates. Our initial tests indicate that the use of large high-powered sonicators in the CSTR mode can result in viable degradation efficiencies.

An attractive alternative to the flow-through probe system is the high-intensity flat-plate reverberatory sonicator or the near-field acoustical processor (NAP).[40] The NAP reactor system consists of two sonicated metal plates that form two sides of a rectangular flow-through pipe; one plate has a set of transducers operated at 16 kHz while the opposing plate has a similar set of

(37) Witte, F.; Urbanik, E.; Zetzsch, C. *J. Phys. Chem.* **1986**, *90*, 325.
(38) (a) Seddow, W. A.; Fletcher, J. W.; Sopchyshyn, F. C. *Can. J. Chem.* **1973**, *51*, 1123. (b) Burkholder, J. B.; Hammer, P. D.; Howard, C. J. *J. Phys. Chem.* **1987**, *91*, 2136.
(39) Mills, G.; Chew, B.; Hoffmann, M. R. Photocatalytic Degradation of Pentachlorophenol on TiO_2. Manuscript in preparation.
(40) Mason, T. J.; Lorimer, J. P. *Sonochemistry*; Ellis Horwood Limited: Chichester, England, 1988; pp 226–227.

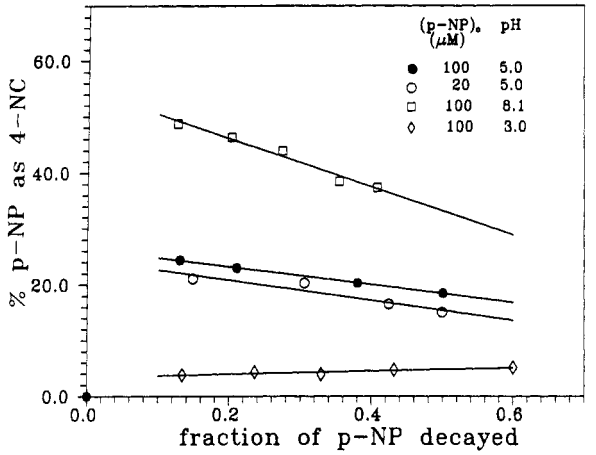

Figure 11. Percentage of PNP decayed converted to 4-NC.

transducers operated at 20 kHz. In this configuration, a liquid flowing between the plates, which may be as large as 0.5 m × 3 m with a plate separation of 0.08 m, is exposed to an ultrasonic intensity that is greater than that expected from a simple doubling of a single plate due to reverberation of the ultrasound. This technology has already been used on a large scale for the extraction of oil from oil shale.[40] In the near future we plan to explore the feasibility of a NAP system for high-capacity water purification. Commercial systems have been constructed to handle process streams with volumetric flow rates approaching 265 L min^{-1}.

Acknowledgment. This research was supported by the U.S. EPA Office of Exploratory Research (Grant Nos. R813326-01-0 and R-815041-01-0).

Appendix

The action of 20-kHz ultrasound on aqueous solutions of PNP resulted in an exponential decrease of [PNP] as shown in Figures 1, 2, and 3. Small amounts of 4-NC were produced as the result of the decay of PNP. The formation of 4-NC led to the quasi-isosbestic point at about 460 nm (Figure 1). The presence of isosbestic points in the absorption spectra of products and reactants implies that, after a certain reaction time, the absorption of unreacted PNP plus the absorption of all products is, at a particular wavelength, equal to the initial absorption of the PNP solution. This condition is represented by eq a1 (for l = 1 cm), where

$$([PNP]_0 - [PNP]_t)\epsilon^{460}_{p\text{-}np} = \sum_i([P_i]_t\epsilon^{460}_{p_i}) \qquad (a1)$$

$[PNP]_0$ and $[PNP]_t$ are the concentrations of PNP at reaction times 0 and t, respectively; and $\epsilon^{460}_{p_i}$ is the extinction coefficient of PNP at 460 nm. Similarly, $[P_i]_t$ represents the concentration of the product i after a reaction time t and $\epsilon^{460}_{p_i}$ is the extinction coefficient of product i at 460 nm. Since identical [PNP]'s were obtained from analyses in basic and in acid solutions (at 401 and 317 nm, respectively), it can be assumed that 4-NC is the only product which absorbs above 400 nm in alkaline solutions. If the term in parentheses on the left-hand side of eq a1 is substituted by $\Delta[PNP]_t$, then the equation can be rearranged to eq a2. In eq a2, $\Delta[PNP]_t$ is the amount of PNP which has disappeared after

$$100\frac{\epsilon^{460}_{PNP}}{\epsilon^{460}_{4\text{-}NC}} = 100\frac{[4\text{-}NC]_t}{\Delta[PNP]_t} = P \qquad (a2)$$

a sonication time t and $[4\text{-}NC]_t$ represents the concentration of 4-NC formed after the same period of time. Hence, the term on the right-hand side of this equation corresponds to the percentage (P) of decomposed PNP which has been converted into 4-NC, after a reaction time t. According to eq a2, this percentage should remain constant with reaction time if an isosbestic point is to be observed. From ϵ^{460}_{PNP} = 1600 M^{-1} cm^{-1} and $\epsilon^{460}_{4\text{-}NC}$ = 7300 M^{-1} cm^{-1} (in 0.1 M NaOH) it is calculated by eq a2 that about 22% of the reacted PNP was converted to 4-NC in a 100 μM solution of PNP sonicated at pH = 5. In order to verify the validity of the assumptions which led to eq a2, calculation of P was made from the known concentrations of 4-NC and PNP at different reaction times. To allow for an easy comparison of results obtained under different conditions, the values of P were plotted as function of the fraction of PNP destroyed (F) instead of sonication time (Figure 11). Line 1 in Figure 11 shows the evolution of P with reaction times for a 100 μM solution of PNP sonicated at pH = 5. P decreased slightly with increasing F; when only small amounts of PNP have decayed (F = 0.13) the fraction P is 24.5% whereas after one half-life (F = 0.5) P amounts to 19%. The results presented in line 1 of Figure 11 help to explain the small shifts toward longer λ, with increasing sonication times, of the point where the spectrum of the unsonicated solution is intersected by the spectrum of the sonicated solution. As P decreased slightly with increasing F, eq 23 predicts a shift of the intersection point toward longer wavelengths, since ϵ^{460}_{PNP} decreases but $\epsilon^{\lambda}_{4\text{-}NC}$ increases with increasing λ. Because of the large difference in the extinction coefficients of PNP and 4-NC the shifts in the intersection points were very small, resulting in a broad ($\Delta\lambda \simeq 2$ nm) isosbestic point centered at 460 nm. Note that the "mean" value of P in line 1 of Figure 11 is 22%, in good agreement with the calculation using eq a2. The quasi-isosbestic points were close to 460 nm for the experiments carried out at pH = 5. This is not surprising since, at $[PNP]_i < 1$ mM, the dependence of P on F did not change appreciably by changing $[PNP]_i$. An example of this is the result obtained by sonication of a 20 μM solution of PNP (line 2 in Figure 11). Only at $[PNP]_i$ = 1 mM the quasi-isosbestic point shifted to shorter wavelengths because P increased to about 30%. Sonication of PNP solutions at pH = 8.1 led to an isosbestic point at $\lambda \simeq 455$ nm. From the extinction coefficients at that wavelength (ϵ_{PNP} = 2700 M^{-1} cm^{-1} and $\epsilon_{4\text{-}NC}$ = 6400 M^{-1} cm^{-1}) it is calculated that P = 42%, whereas the mean value of P in Figure 11 is about 43%. At pH = 3, P is essentially independent of F and $P \simeq 5\%$ (Figure 11, line 4). From the extinction coefficients at the quasi-isosbestic point at 370 nm (ϵ_{PNP} = 530 M^{-1} cm^{-1}, $\epsilon_{4\text{-}NC}$ = 8700 M^{-1} cm^{-1}) a mean value of P = 6% is derived. These examples are a further confirmation of our explanation of the isosbestic points and provide support for the assumption that no product other than 4-NC interfered with the spectrophotometric determinations of [PNP]. This conclusion, in turn, implies that the exponential decay of PNP with sonication time is not an artifact of the analytical methods. The exponential increase of $[NO_2^-]$ with sonication time (Figure 4, curve 1) is also consistent with this conclusion.

Registry No. PNP, 100-02-7; 4-NC, 3316-09-4; •OH, 3352-57-6.